Communication: The origin of rotational enhancement effect for the reaction of H2O+ + H2 (D2)

Anyang Li, Yongle Li, Hua Guo, Kai-Chung Lau, Yuntao Xu, Bo Xiong, Yih-Chung Chang, and C. Y. Ng

Citation: The Journal of Chemical Physics **140**, 011102 (2014); doi: 10.1063/1.4861002
View online: http://dx.doi.org/10.1063/1.4861002
View Table of Contents: http://scitation.aip.org/content/aip/journal/jcp/140/1?ver=pdfcov
Published by the AIP Publishing

Communication: The origin of rotational enhancement effect for the reaction of $H_2O^+ + H_2$ (D_2)

Anyang Li,[1] Yongle Li,[1] Hua Guo,[1,a)] Kai-Chung Lau,[2] Yuntao Xu,[3] Bo Xiong,[3] Yih-Chung Chang,[3] and C. Y. Ng[3,b)]
[1]*Department of Chemistry and Chemical Biology, University of New Mexico, Albuquerque, New Mexico 87131, USA*
[2]*Department of Biology and Chemistry, City University of Hong Kong, Kowloon, Hong Kong*
[3]*Department of Chemistry, University of California, Davis, California 95616, USA*

(Received 14 November 2013; accepted 19 December 2013; published online 6 January 2014)

We have measured the absolute integral cross sections (σ's) for H_3O^+ formed by the reaction of rovibrationally selected $H_2O^+(X^2B_1;\ v_1^+v_2^+v_3^+ = 000;\ N^+_{Ka}{}^+_{Kc}{}^+ = 0_{00},\ 1_{11}$, and 2_{11}) ion with H_2 at the center-of-mass collision energy (E_{cm}) range of 0.03–10.00 eV. The $\sigma(0_{00})$, $\sigma(1_{11})$, and $\sigma(2_{11})$ values thus obtained reveal rotational enhancements at low $E_{cm} < 0.50$ eV, in agreement with the observation of the previous study of the $H_2O^+(X^2B_1) + D_2$ reaction. This Communication presents important progress concerning the high-level *ab initio* quantum calculation of the potential energy surface for the $H_2O^+(X^2B_1) + H_2$ (D_2) reactions, which has provided valuable insight into the origin of the rotational enhancement effect. Governed by the charge and dipole-induced-multipole interactions, the calculation shows that H_2 (D_2) approaches the H end of $H_2O^+(X^2B_1)$ in the long range, whereas chemical force in the short range favors the orientation of H_2 (D_2) toward the O side of H_2O^+. The reorientation of H_2O^+ reactant ion facilitated by rotational excitation thus promotes the $H_2O^+ + H_2$ (D_2) reaction along the minimum energy pathway, rendering the observed rotational enhancement effects. The occurrence of this effect at low E_{cm} indicates that the long range charge and dipole-induced-multipole interactions of the colliding pair play a significant role in the dynamics of the exothermic $H_2O^+ + H_2$ (D_2) reactions. © *2014 AIP Publishing LLC*. [http://dx.doi.org/10.1063/1.4861002]

Understanding of mode specificity in reaction dynamics is of fundamental importance.[1–6] However, despite many recent advances, systematic investigations of mode specificity are still relatively rare, largely because of difficulties associated with the preparation of the reactant quantum state and with the control of the translational energy. The recent advances in preparing single rovibrational states of the water cation, H_2O^+,[7,8] using the newly developed vacuum ultraviolet (VUV) laser pulsed field ionization-photoion (PFI-PI) method[9–11] has enabled detailed experimental studies of the influence of the H_2O^+ rotational and vibrational modes as well as the translational energy on its reaction with D_2, leading to the $D + H_2DO^+$ products. The absolute integral reaction cross sections (σ's) obtained at the center-of-mass collision energy (E_{cm}) range of 0.03–10.00 eV indicate a monotonic decay with E_{cm}, implying an exothermic, barrierless reaction pathway.[7,8] These state-resolved experimental results also suggested that the rotational excitation of the H_2O^+ reactant ion significantly enhances the reactivity, particularly at low E_{cm} values (<0.50 eV). On the other hand, the excitation of the vibrational modes of H_2O^+ has relatively small effects. Considering that the rotation energy involved is small (<200 cm^{-1}), it is intriguing to find a substantial effect on the chemical reactivity of H_2O^+. These experimental results represent a complete set of quantum state resolved data for a prototypical ion-molecule reaction, which provides strong impetus for a first-principles characterization of the reaction dynamics and mode specificity. Indeed, given the small number of electrons (11), an accurate description of the electronic structure is well within the reach of state-of-the-art *ab initio* methods. A full-dimensional quantum mechanical characterization of the reaction dynamics is also feasible, but requiring a nine-dimensional global potential energy surface (PES).

This Communication reports on important progress concerning extensive *ab initio* calculations of the reaction path for the titled reaction, which have provided significant insight into the nature of the observed rotational enhancement[7,8] for the $H_2O^+(X^2B_1;\ v_1^+v_2^+v_3^+;\ N^+_{Ka}{}^+_{Kc}{}^+) + D_2$ reactions. As a concerted experimental effort to further support the theoretical inquiry, we have also measured the σ values for the reaction of $H_2O^+(X^2B_1;\ v_1^+v_2^+v_3^+ = 000;\ N^+_{Ka}{}^+_{Kc}{}^+ = 0_{00},\ 1_{11}$, and $2_{11}) + H_2$, which are presented here for comparison with those reported previously for the $H_2O^+(X^2B_1) + D_2$ reaction.

The σ measurement for the rovibrationally selected $H_2O^+(X^2B_1) + H_2$ reaction was conducted by employing the VUV laser PFI-PI double-quadrupole-double-octopole apparatus, which has been reported in detail previously.[7–11] Briefly, the apparatus consists of, in sequential order, a molecular beam source for the generation of a pulsed supersonic H_2O beam, a VUV laser PFI-PI ion source for the preparation of a state-selected reactant $H_2O^+(X^2B_1;\ v_1^+v_2^+v_3^+;$

a)Email: hguo@unm.edu
b)Email: cyng@ucdavis.edu

$N^+{}_{Ka}{}^+{}_{Kc}{}^+$) ion beam, a reactant quadrupole mass spectrometer (QMS) for the selection of reactant ions, a set of dual radio frequency (rf) octopole ion guides for confining and guiding the reactant and product ions, a reactant gas cell, where the $H_2O^+ + H_2$ reaction occurs, a product QMS for the selection of reactant and product ions, and a Daly-type detector for ion detection. The experimental procedures are similar to those described previously in the $H_2O^+ + D_2$ study.[7–11] Tunable VUV laser radiation in the range of 101 600–102 025 cm^{-1} for the preparation of state-selected $H_2O^+(X^2B_1; v_1{}^+v_2{}^+v_3{}^+ = 000; N^+{}_{Ka}{}^+{}_{Kc}{}^+ = 0_{00}, 1_{11}$, and 2_{11}) reactant ion from H_2O was generated by four-wave sum-frequency mixing using Xe gas in the form of a pulsed jet as the nonlinear medium.[6,7] By employing a pulsed electric field scheme to the VUV-PFI-PI source, we have shown that a rovibrationally selected $H_2O^+(X^2B_1; v_1{}^+v_2{}^+v_3{}^+ = 000; N^+{}_{Ka}{}^+{}_{Kc}{}^+ = 0_{00}, 1_{11}$, and 2_{11}) PFI-PI ion beam can be prepared with not only high internal state-purity and high intensity but also high resolution in laboratory kinetic energy (E_{lab}) for collisional studies. The narrow E_{lab} spread ($\Delta E_{lab} = \pm 0.05$ eV) achieved for the PFI-PI ion beam only contributes to a spread of ± 0.005 eV for the ΔE_{cm} spread of the titled reaction;[7,8] and thus allows the σ measurement to cover the full E_{cm} range 0.03–10.00 eV that is of chemical interest. The reactant H_2 gas sample (purity = 99.9%) was purchased from Sigma Aldrich. The H_2 pressure used in the reaction cell was 1.0×10^{-4} Torr, which was monitored by a MKS Baratron. All experimental σ values presented here represent the average values of at least three independent measurements; and the run-to-run uncertainties were found to be about 10%. The systematic errors on the experimental σ values are estimated to be 30%.[7–11]

The σ values for the $H_2O^+(X^2B_1; v_1{}^+v_2{}^+v_3{}^+ = 000; N^+{}_{Ka}{}^+{}_{Kc}{}^+ = 0_{00}, 1_{11}$, and $2_{11}) + H_2$ reaction measured at $E_{cm} = 0.03$–10.00 eV are plotted in Fig. 1(a) for comparison with those reported previously[7,8] for the $H_2O^+(X^2B_1; v_1{}^+v_2{}^+v_3{}^+ = 000; N^+{}_{Ka}{}^+{}_{Kc}{}^+ = 0_{00}, 1_{11}$, and $2_{11}) + D_2$ reaction shown in Fig. 1(b). The dotted curves shown in Figs. 1(a) and 1(b) are the predictions based on the Langevin-Gioumousis-Stevenson (LGS) capture model.[12] Although the general profiles of the experimental σ curves for the $H_2O^+ + H_2$ and $H_2O^+ + D_2$ reactions are consistent with the predictions of the LGS model, we find the σ values for $H_2O^+ + H_2$ reaction at $E_{cm} < 1.00$ eV to be significantly higher than those for the $H_2O^+ + D_2$ reaction. Due to the importance of the H_2O^+ and H_2 reaction in astrophysics, the thermal rate constants of the $H_2O^+ + H_2$ reaction have been measured using various experimental techniques[13–17] in the past decades. The estimated σ values converted from the reported thermal rate constants are included in Fig. 1(a). The large discrepancy observed in these rate constant measurements justifies the present σ measurement of the reaction.

The most important feature of concern to this study is the identification of the rotational enhancement effect for the $H_2O^+ + H_2$ (D_2) reactions. As shown in Fig. 1(a), the rotational selected cross section curves at $E_{cm} < 0.50$ eV are found to have the order, $\sigma(0_{00}) < \sigma(1_{11}) < \sigma(2_{11})$; and this observation is in excellent accord with that shown in Fig. 1(b). The rotational enhancement for $H_2O^+ + H_2$ seems

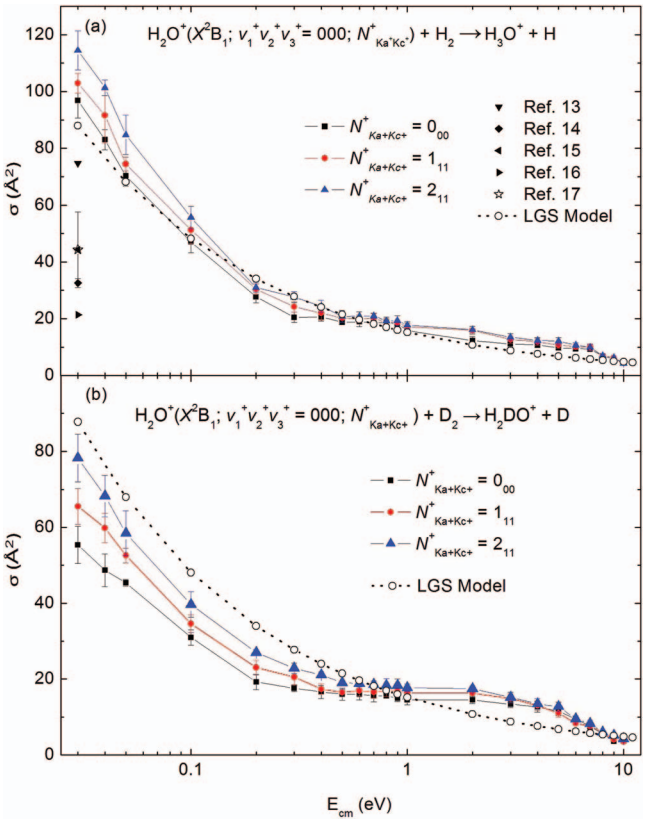

FIG. 1. Comparison on the σ values in Å^2 of the reactions between $H_2O^+(X^2B_1; v_1{}^+v_2{}^+v_3{}^+ = 000; N^+{}_{Ka}{}^+{}_{Kc}{}^+ = 0_{00}, 1_{11}$, and 2_{11}) and (a) H_2 and (b) D_2 in the E_{cm} range of 0.03–10.00 eV. The predictions based on the LGS orbiting model are shown in (a) and (b) as the dotted curves. The estimated σ values converted from thermal rate constants for the $H_2O^+ + H_2$ reaction reported previously in Refs. 13–17 are also included in (a).

to be less pronounced than that observed for $H_2O^+ + D_2$. We have pointed out in previous studies that the ΔE_{cm} spread in the present experiment is predominantly governed by the thermal motion of the H_2 in the gas cell at a temperature of 298 K.[7,8] For $E_{cm} = 0.03$, 0.04, 0.05, 0.10, and 0.50 eV, the respective ΔE_{cm} values are predicted to be 0.08, 0.10, 0.11, 0.15, and 0.34 eV. Since ΔE_{cm} is greater than E_{cm} at $E_{cm} < 0.15$ eV, the measured σ values at E_{cm} lower than 0.15 eV might be distorted.[7,8] However, this would not alter the conclusion of identifying the rotational enhancement for the titled reaction.

To better understand the experimental observations, we have performed high-level *ab initio* calculations on the title reaction. All calculations were carried out using an explicitly correlated version of the unrestricted coupled cluster singles, doubles, and perturbative triples (UCCSD(T)-F12b) method[18,19] with the augmented correlation-consistent polarized valence triple-zeta (aug-cc-pVTZ or AVTZ) basis set. The explicit treatment of the electron-electron interaction allows the fast convergence with respect to the complete basis set limit using AVTZ.[20] Such an approach has recently been shown to provide accurate descriptions of many molecular properties,[18,19,21] including global PESs.[22,23] The MOLPRO suite of electronic structure programs[24] was used in all calculations.

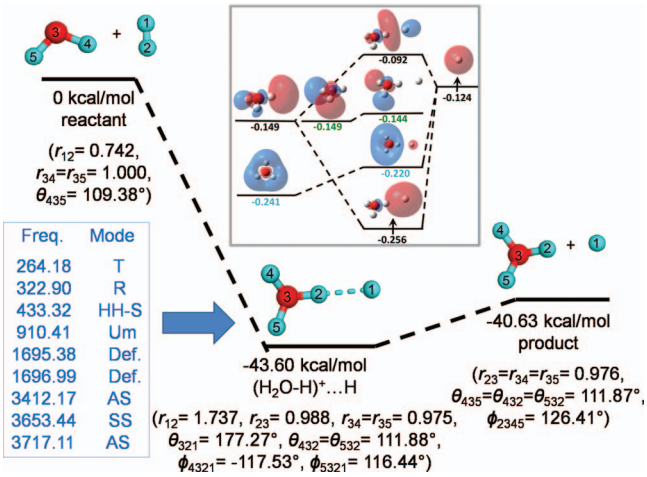

FIG. 2. Calculated energetics of the $H_2O^+ + H_2 \rightarrow H_3O^+ + H$ reaction path in kcal/mol. The *ab initio* energies and geometries of the stationary points are given in the figure (bond lengths are in Å and bond angles are in degree). The normal mode frequencies (cm^{-1}) for the H_4O^+ complex are also given: T (twist), R (rock), HH-S (H1-H2 stretch), U (umbrella), D (deformation), B (bend), SS (symmetric stretch), and AS (antisymmetric stretch). The molecular orbital energy level diagram for the H_4O^+ ion is given in the inset.

Figure 2 shows the calculated energetics of the $H_2O^+ + H_2 \rightarrow H_3O^+ + H$ reaction path. The *ab initio* energies and geometries of the stationary points are given in the figure with the bond lengths in Å and the angles in degree. The harmonic frequencies (cm^{-1}) of the H_3O^+ intermediate are also given. This reaction has no intrinsic barrier (*vide infra*), consistent with the measured monotonically decaying trend of the σ curve or excitation function reported here and in Refs. 7 and 8. The theoretical exothermicity of 1.76 eV (1.61 eV with zero point energy correction) obtained is in agreement with the known experimental exothermicity of 1.72 eV.[7,8] A potential energy minimum is predicted along the reaction path, which has a well-depth of 0.13 eV with respect to the $H_3O^+ + H$ channel. The corresponding $H_3O^+\cdots H$ complex is due to a weak single-electron bond (hemibond), which arises from the interaction between the H atom and lowest unoccupied molecular orbitals (LUMOs) of H_3O^+. As shown in the inset of Fig. 2, the singly occupied molecular orbital (SOMO) of H is close in energy to the two (LUMOs) of H_3O^+, and their interaction results in a MO that is lower in energy than of the SOMO of H, according to spin-restricted open shell density functional theory (RO-DFT) calculations using the MPW1K functional[25] with the 6–311++G(d) basis set. The population of this MO leads to a shallow potential well for the $(H_3O)^+\cdots H$ complex. The nature of this interaction is similar to that between halogen and water.[26]

Due to the barrierless nature of the reaction, the reactivity is largely determined by the entrance channel of the PES. To this end, we have mapped out the minimum energy path (MEP) in two coordinates. The first is the bond length of the H_2 reactant, namely the H1-H2 distance. The second one is the distance between O of H_2O^+ and the hydrogen atom H2 in H_2 that is closer to O, i.e., the O-H2 distance. All other bond lengths and angles are optimized. Totally, 118 points were used to map out the two-dimensional-MEP shown in the upper panel of Fig. 3. Six optimized structures are marked as

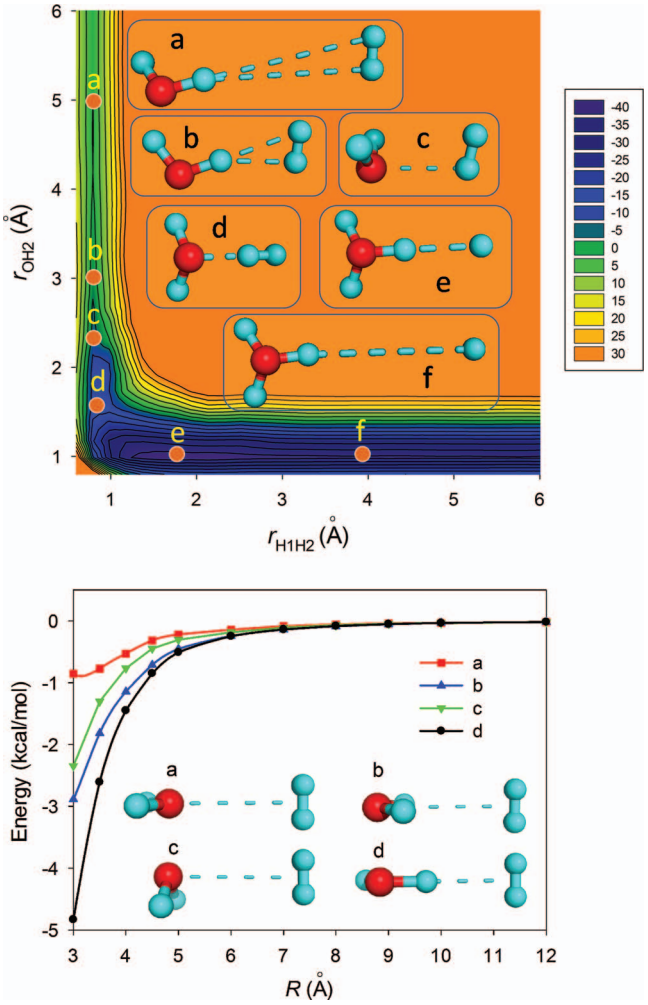

FIG. 3. (Upper panel) Contour plot of the minimum energy path (MEP) along the H1-H2 and O-H2 distances with all other internal coordinates optimized. Energies are in kcal/mol relative to the reactants. Five optimized structures are marked along the reaction path. (Lower panel) Asymptotic potential energy curves calculated in the distance between atom O and the center-of-mass of hydrogen molecular with the reactants fixed at their equilibrium geometries. Four relative orientations (a)–(d) are considered.

(a)–(f) along the barrierless reaction path and their configurations are displayed in the figure. In the reactant asymptote, the reaction coordinate is primarily the O-H2 distance, due to the long-range electrostatic interactions, including the charge-induced dipole, charge-quadrupole, dipole-quadrupole, and dipole-induced dipole interactions. In the lower panel of Fig. 3, the long-range potential energy curves are shown between the two reactants with fixed equilibrium geometries and orientations. Although all approaches are barrierless, the most attractive orientation is the one with H_2 approaches the H end of H_2O^+ perpendicular to its molecular plane. However, this most attractive approach does not result directly in reaction. As the two species become closer, the short-range chemical force dictates that H2 interacts with the O end, rather than the H end, of the H_2O^+ ion, in order to produce the H_3O^+ product ion. This change of orientation is almost certainly responsible for the increased reaction cross section when H_2O^+ is rotationally excited. Beyond the O-H2 distance $r_{OH2} = 3$ Å, the reaction coordinate is dominated by the H1-H2 distance. The potential leads to the $(H_3O)^+\cdots H$ well, which is −1.89 eV

relative to the reactants. Further increasing the H1-H2 distance leads to the $H_3O^+ + H$ product channel.

These UCCSD(T)-F12b/AVTZ calculations reported here pave the way for the determination of the global PES of this reactive system. Due to its high dimensionality (9), a large number of *ab initio* points evenly distributed along the reaction path will be needed. Fitting of the *ab initio* points in a large configuration space with high fidelity will be a challenge, but recent advances in fitting reactive PESs with neural networks,[23,27] particularly those that adapt the permutation symmetry,[28,29] will be ideally suited for constructing the high-dimensional PES for the title reaction. Such a PES will allow both quantum mechanical and quasi-classical trajectory studies of the reaction dynamics and further elucidate the mode specificity in this system.

This work is supported by the Department of Energy (DE-FG02-05ER15694 to H.G.) and (DE-FG02-02ER15306 to C.Y.N.). C.Y.N. also acknowledges partial support by the NASA Planetary Atmospheres Program Grant No. 07-PATM07-0012. K.-C.L. thanks the support by a Strategic Research Grant from City University of Hong Kong (Project No. 7004019).

[1]J. C. Polanyi, Acc. Chem. Res. **5**, 161 (1972).
[2]R. N. Zare, Science **279**, 1875 (1998).
[3]F. F. Crim, Acc. Chem. Res. **32**, 877 (1999).
[4]S. L. Anderson, Adv. Chem. Phys. **82**, 177 (1992).
[5]C. Y. Ng, J. Phys. Chem. A **106**, 5953 (2002).
[6]S. Yan, Y.-T. Wu, and K. Liu, Proc. Natl. Acad. Sci. U.S.A. **105**, 12667 (2008).
[7]Y. Xu, B. Xiong, Y. C. Chang, and C. Y. Ng, J. Chem. Phys. **137**, 241101 (2012).
[8]Y. Xu, B. Xiong, Y. C. Chang, and C. Y. Ng, J. Chem. Phys. **139**, 024203 (2013).
[9]Y. C. Chang, H. Xu, Y. Xu, Z. Lu, Y.-H. Chiu, D. J. Levandier, and C. Y. Ng, J. Chem. Phys. **134**, 201105 (2011).
[10]Y. C. Chang, Y. Xu, Z. Lu, H. Xu, and C. Y. Ng, J. Chem. Phys. **137**, 104202 (2012).
[11]Y. Xu, Y. C. Chang, Z. Lu, and C. Y. Ng, Astrophys. J. **769**, 72 (2013).
[12]G. Gioumousis and D. P. Stevenson, J. Chem. Phys. **29**, 294 (1958)
[13]F. C. Fehsenfeld, A. L. Schmelikeope, and E. E. Ferguson, J. Chem. Phys. **46**, 2802 (1967).
[14]J. K. Kim, L. P. Theard, and W. T. Huntress, Jr., J. Chem. Phys. **62**, 45 (1975).
[15]I. Dotan, W. Lindinger, B. Rowe, D. W. Fahey, F. C. Fehenfeld, and D. L. Albritton, Chem. Phys. Lett. **72**, 67 (1980).
[16]A. B. Rakshit and P. Warneck, J. Chem. Phys. **74**, 2853 (1981).
[17]J. D. C. Jones, K. Birkinshaw, and N. D. Twiddy, Chem. Phys. Lett. **77**, 484 (1981).
[18]T. B. Adler, G. Knizia, and H.-J. Werner, J. Chem. Phys. **127**, 221106 (2007).
[19]G. Knizia, T. B. Adler, and H.-J. Werner, J. Chem. Phys. **130**, 054104 (2009).
[20]D. Feller and K. A. Peterson, J. Chem. Phys. **139**, 084110 (2013).
[21]T. Shiozaki and H.-J. Werner, Mole. Phys. **111**, 607 (2013).
[22]J. Li, Y. Wang, B. Jiang, J. Ma, R. Dawes, D. Xie, J. M. Bowman, and H. Guo, J. Chem. Phys. **136**, 041103 (2012).
[23]J. Chen, X. Xu, X. Xu, and D. H. Zhang, J. Chem. Phys. **138**, 221104 (2013).
[24]H.-J. Werner, P. J. Knowles, G. Knizia, F. R. Manby, M. Schütz *et al.*, MOLPRO, version 2010.1, a package of *ab initio* programs, 2010, see http://www.molpro.net.
[25]B. J. Lynch, P. L. Fast, M. Harris, and D. G. Truhlar, J. Phys. Chem. A **104**, 4811 (2000).
[26]J. Li, Y. Li, and H. Guo, J. Chem. Phys. **138**, 141102 (2013).
[27]L. M. Raff, R. Komanduri, M. Hagan, and S. T. S. Bukkapatnam, *Neural Networks in Chemical Reaction Dynamics* (Oxford University Press, Oxford, 2012).
[28]B. Jiang and H. Guo, J. Chem. Phys. **139**, 054112 (2013).
[29]J. Li, B. Jiang, and H. Guo, J. Chem. Phys. **139**, 204103 (2013).